

## Optimized multi-objective design of herringbone micromixers

Cesar A. CORTES-QUIROZ <sup>1,\*</sup>, Mehrdad ZANGENEH <sup>1</sup>

\* Corresponding author: Tel.: ++44 (0)2076 793997; Fax: ++44 (0)2073 880180;  
Email: c\_cortesqurz@meng.ucl.ac.uk

1: Department of Mechanical Engineering, University College London, UK

**Abstract** A design method which systematically integrates Computational Fluids Dynamics (CFD) with an optimization scheme based on the use of the techniques Design of Experiments (DOE), Function Approximation technique (FA) and Multi-Objective Genetic Algorithm (MOGA), has been applied to the shape optimization of the staggered herringbone micromixer (SHM) at different Reynolds numbers. To quantify the mixing intensity in the mixer a Mixing index is defined on the basis of the intensity of segregation of the mass concentration on the outlet section. Four geometric parameters, i.e., aspect ratio of the mixing channel, ratio of groove depth to channel height, ratio of groove width to groove pitch and the asymmetry factor (offset) of groove, are the design variables selected for optimization. The mixing index at the outlet section and the pressure drop in the mixing channel are the performance criteria used as objective functions. The Pareto front with the optimum trade-offs, maximum mixing index with minimum pressure drop, is obtained. Experiments for qualitative and quantitative validation have been implemented.

**Keywords:** Herringbone Micromixer, Multi-objective Optimization, Design of Experiments, Genetic Algorithm

### 1. Introduction

In recent years, microfluidics systems have been increasingly applied to perform many functions such as separation, mixing, reaction, synthesis and analysis on a single chip widely known as lab-on-a-chip. The development of this micro device concept and technology has been rapid to find its use in the sorting of cells, drug delivery, chemical and enzyme reactions, the synthesis of nucleic acids and the analysis of DNA and proteins. An important factor that determines the performance of these microfluidics systems is their mixing efficiency which is critical in several applications, e.g. fast chemical reactions.

In a microscopic domain the Reynolds number is low and flow is restricted to the laminar regime. Molecular diffusion becomes the dominant mixing mechanism which is very slow and consequently increases the length of micro-channels and time required for complete mixing. Micromixers are the components that have been developed to achieve fast mixing in lab-on-a-chip and bio-MEMS systems. Their design is based on the achievement of three basic processes of fluids

mixing: molecular diffusion, stretching and folding and breakup (Ottino 1989). A number of micromixers designs have been reported in the literature and they can be classified into active and passive micromixers (Nguyen and Wu 2005, Hessel et al 2005). Active mixers induce turbulent flows either by using moving parts or an external source of energy such as an electric field, magnetic field, pressure, etc. Passive mixers do not have an extra forcing mechanism and mixing is achieved by creating a transverse flow through modification of their geometries.

Passive micromixers have been preferred in most applications due to their simple design, easiness of fabrication and integration compared to active ones. One of the passive methods to enhance the mixing process is to place microstructured objects on one or more walls of the channel. One of these designs, the staggered herringbone micromixer (SHM), was initially proposed by Stroock et al (2002) and has been found to give good mixing performance at low Reynolds numbers ( $Re < 10$ ) and low resistance to flow. This design has alternating cycles of asymmetric herringbone shaped grooves on the floor of the

channel through which transverse flow is produced as a result of the reduced pressure gradient present there.

Several numerical studies have been carried out on the SHM with the aim of understanding the mixing mechanism and the effect of various geometrical parameters on the mixing quality. Stroock and McGraw (2004) approximated the complex three-dimensional flow field using a two dimensional lid-driven cavity model that was tuned to provide qualitative agreement to experimental data and studied the effect of varying two geometric parameters: the asymmetry or offset of the groove and the number of grooves in each cycle; Liu et al (2004) studied the influence of different fluid properties and a large concentration gradient on mixing at  $Re = 1$  and  $10$  for a fixed geometry; Aubin et al (2003, 2005) investigated numerically the effect of three geometric parameters: the groove depth, the groove width and the number of grooves per cycle, using a particle tracking method to visualize and quantify the mixing performance; Kang and Kwon (2004) studied the mixing performance of three types of grooved micromixers including the SHM; Yang *et al* (2005) studied the effects of varying herringbone groove offset, depth, and angle, as well as the ratio of inlet channel width to mixing channel width by applying CFD to nine configurations defined with an array given by the Taguchi method; Li and Chen (2005) used the Lattice Boltzmann method to study numerically the effect on mixing performance of the asymmetry factor and the number of grooves per half cycle; Hassel and Zimmerman (2006) presented a numerical study of the flow through the SHM to characterize the effect of the grooves on moving fluid across the channel, in particular of the groove depth in  $Re$  range of  $0-15$  and of the number of grooves per half cycle; Lynn and Dandy (2007) evaluated numerically the generation of helical flows over patterned grooves and its optimization i.e. the increment of transverse flow, by varying the ratio of the length of the grooves to the neighbouring ridge for a given groove depth and channel aspect ratio of the slanted groove micromixer and

discussed the implications of translating the optimized parameters to the SHM design; Ansari and Kim (2007a, 2007b) used a numerical procedure that combines three-dimensional Navier-Stokes analysis and numerical optimization tools, the Radial Basis Neural Network (RBNN) method with Sequential Quadratic Programming (SQP) and the Response Surface Method (RSM) to enhance mixing performance by optimizing the groove using the ratio of groove depth to channel height, ratio of groove width to groove pitch and angle of the groove; Singh et al (2008) introduced a new simplified formulation of the mapping method (Kang et al 2008) to make it much simpler to implement and applied the method to optimize three micromixer designs including the SHM for which groove depth and number of grooves per half cycle were used as parameters.

It is clear that mixing in the SHM can be effectively increased by optimizing the shape of the grooves and channel. As cited above, previous work has already investigated on the effects of geometric parameters on mixing, but there have been few attempts of using systematically automatic optimization techniques for designing and all of them have been based on the optimization of only the mixing performance. However, in most problems of practical interest multi-objective criteria need to be met e.g. mixing versus pressure loss or energy consumption or dissipation or residence time.

In this paper, a design and optimization methodology is applied to the SHM. It systematically integrates CFD with an optimization strategy based on the use of Design of Experiments (DOE), Function Approximation (FA) and Multi-Objective Genetic Algorithm (MOGA) techniques. Bonaiuti and Zangeneh (2006) applied this multi-objective approach to the design of turbomachinery components. The effect on mixing of selected geometric parameters of the SHM have been evaluated and the parameters optimized accordingly. The goal of the optimization is to obtain the configurations that provide the maximum mixing index with lowest pressure drop.

## 2. Optimization methodology

A schematic diagram of the methodology used for the optimization of the SHM is shown in figure 1. The process starts with the selection of design parameters and their range of variation as well as the performance parameters to be evaluated. With the design parameters defined, the Design of Experiment (DOE) method is used to create the experimental table which corresponds to different geometries representing the design space. These geometries need to be evaluated then by CFD to compute the performance parameters. Once the flow field in all configurations is computed the Function Approximation (FA) or surrogate model can be used to define an approximated response function or surface that relates the performance parameters to design parameters. The accuracy of the response surface is a critical step in the design process and once this is established the response surface can be used to carry out sensitivity analysis in order to establish the most critical design parameters. Finally, a Multi-objective Genetic Algorithm (MOGA) is run on the response surface. The response surface enables the user to evaluate the objective function without the requirement to carry out expensive CFD evaluation for each configuration. This makes the application of MOGA a practical reality and enables the user to be able to see the optimum boundary of the trade-offs between different design objectives in the design space, the Pareto front (Pf).

### 2.1. Selection of performance and design parameters

The performance parameters defined for this study are the mixing quality and the pressure drop in the channel. In order to measure and compare the mixing intensity using the outputs from CFD code, a Mixing index is defined based on mass concentration distribution. In this study, the definition of mixing index is based on the intensity of segregation introduced by Danckwerts (1952) and is calculated by equation 1:

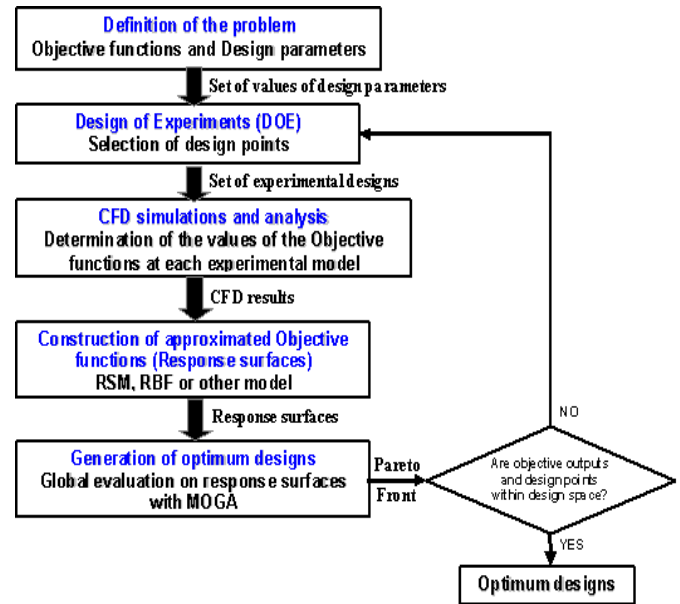


Fig. 1. Flowchart of the methodology process.

$$Mi = 1 - \sqrt{\frac{\int_A (c - \bar{c})^2 dA}{A \cdot \bar{c} (1 - \bar{c})}} \quad (1)$$

where  $c$  is the concentration distribution at the selected cross-section plane (in this study, it is the outlet plane at the end of the mixing channel),  $\bar{c}$  is the averaged value of the concentration field on the plane and  $A$  is the area of the plane.  $Mi$  reaches a value of 0 for a complete segregated system and a value of 1 for the homogeneously mixed case. The mass concentration information from CFD analyses is used in equation 1.

The second performance parameter is the pressure loss in the mixing channel which is evaluated by the difference between the area weighted average of total pressure on the outlet plane and on a cross section plane at the inlet of the mixing channel.

Fig. 2 displays the geometric dimensions in the SHM that can be used for the design parameterization. For all the models prepared in this study, the mixing channel length is 3 mm in which three half cycles of periodic grooves are defined. With the conclusions of previous work cited in the introduction section on mixing in the SHM and by making an initial sensitivity analysis of the influence of design parameters on the mixing index working with a small set of SHM

configurations, the design parameters to complete the optimization procedure are: aspect ratio of the mixing channel,  $W/h$ , ratio of groove depth to channel height,  $d/h$ , ratio of groove width to groove pitch,  $w_g/D$ , and the asymmetry factor,  $p$ . The following geometric features are fixed: width of the mixing channel,  $W = 200 \mu\text{m}$ , groove pitch,  $D = 100 \mu\text{m}$ , angle of the groove,  $\theta = 90^\circ$ , number of grooves per half cycle,  $N_g = 6$ , and width of inlet channels,  $U = 100 \mu\text{m}$ .

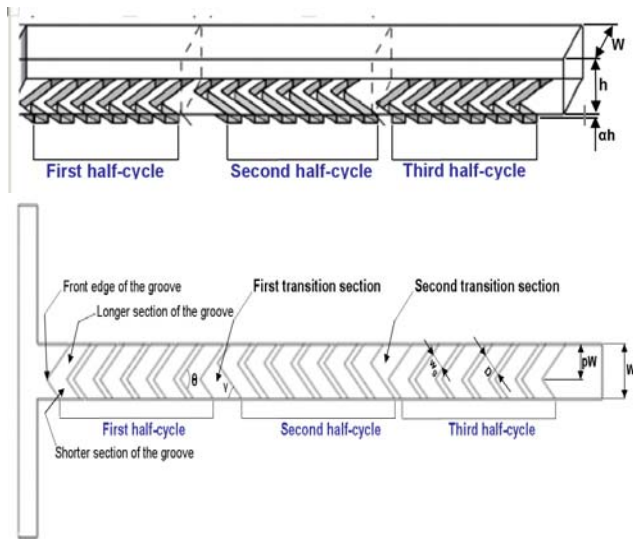


Fig. 2. Geometric dimensions of the SHM design.

## 2.2. Design of experiments (DOE), the Taguchi method

DOE technique defines a subset of design points (experiments) from the design space which is representative enough to evaluate the influence of designs parameters on performance parameters.

The Taguchi method (Taguchi 1987) is used in this study. It is based on Orthogonal Array (OA) of experiments and gives much reduced variance for the experiment with optimum settings of design parameters. Table 1 shows the values of the levels adopted by the design parameters in the experiments (designs points) defined by the DOE. These 27 experiments (CFD simulations) are defined in the Taguchi's OA  $L_{27}$  shown in table 2.

## 2.3. Numerical simulations

Numerical simulations of the transport process

in the SHM models are performed to investigate the mixing quality achieved with the geometrical configurations defined by the DOE. The CFD code used for this study is the commercial Navier-Stokes Solver CFX-11 (ANSYS Europe Ltd. 2007) which is based on the Finite Volume Method. The geometries of different configurations were constructed and meshed by using the commercial mesh generator GRIDGEN (Pointwise Inc. 2006).

Table 1  
Design parameters and levels.

Factors <sup>a</sup>	A. $W/h$	B. $d/h$	C. $w_g/D$	D. $p$
1	1.60	0.25	0.25	0.55
2	2.40	0.50	0.50	0.70
3	3.20	0.75	0.75	0.85

<sup>a</sup> Factors are defined in section 2.1.

The flow is defined viscous, isothermal, incompressible, laminar and in steady-state, for which continuity equation (2), momentum equation (3) and species convection-diffusion equation (4) are solved.

$$\nabla V = 0 \quad (2)$$

$$\rho V \nabla V = -\nabla P + \mu \nabla^2 V \quad (3)$$

$$V \nabla c = D \nabla^2 c \quad (4)$$

where  $\rho$  and  $\mu$  are the density and viscosity of the fluid respectively,  $V$  and  $P$  are the velocity and pressure vectors respectively,  $c$  is the mass fraction or concentration of the fluid under analysis and  $D$  is the diffusion coefficient of the fluid in the other fluid. Advection terms in each equation are discretized with a second order differencing scheme which minimize numerical diffusion in the results. The simulations were defined to reach convergence when the normalized residual for the mass fraction fell below  $1 \times 10^{-5}$ .

The boundary condition for the velocity at the inlets is mass inflow so that only the component in the direction of bulk flow exists to have a uniform velocity profile and the other components are zero.

**Table 2**  
Orthogonal array L<sub>27</sub> (design matrix).

Exps. <sup>b</sup>	Factors <sup>a</sup>			
	A	B	C	D
1	1	1	1	1
2	1	1	2	2
3	1	1	3	3
4	1	2	1	2
5	1	2	2	3
6	1	2	3	1
7	1	3	1	3
8	1	3	2	1
9	1	3	3	2
10	2	1	1	2
11	2	1	2	3
12	2	1	3	1
13	2	2	1	3
14	2	2	2	1
15	2	2	3	2
16	2	3	1	1
17	2	3	2	2
18	2	3	3	3
19	3	1	1	3
20	3	1	2	1
21	3	1	3	2
22	3	2	1	1
23	3	2	2	2
24	3	2	3	3
25	3	3	1	2
26	3	3	2	3
27	3	3	3	1

<sup>a</sup> Factors are defined in table 1.

<sup>b</sup> Experiments which correspond to the models used in CFD simulations.

The velocity values at the inlets are equal and give a laminar flow regime with Reynolds numbers approximately equal to 1 and 10 in the mixing channel. Along the walls, non-slip boundary condition is used for the tangential velocity component whereas the normal component is zero. At the outlet end of the mixing channel, a constant pressure

condition (gauge pressure  $P = 0$ ) is specified. Water at 25 °C and ethanol are the fluids used in the study, the boundary conditions for the species balance are mass fractions equal to 0 at the inlet where pure water is fed and equal to 1 at the inlet where ethanol is fed. Flow vector fields, pressure and mass fraction contours from the simulations results are examined to ensure that the boundary conditions are fulfilled.

A variable mesh composed of hexahedral elements is used and arranged to provide sufficient resolution for boundary layers near the fluid-solid interface on the walls of the channels and the grooves. In order to obtain mesh-independent results from the simulations, a preliminary mesh size sensitivity study was carried out to determine the interval size of convergence.

#### 2.4. Response surfaces construction

The values of design parameters  $X_i$  of the SHM models defined in the DOE matrix (table 2) and the performance parameters  $P_j$  (mixing index, pressure drop) which result from the CFD simulations are correlated by approximated functions:

$$P_j = p_j(X_i), i=1 \text{ to } N, j=1 \text{ to } M \quad (5)$$

where  $N$  is the number of design parameters and  $M$  is the number of performance parameters. The Radial Basis Function, RBF (Kansa 1999), has been used to build the approximation of the correlating functions  $p_j$ . The RBF is a two-layered neural network with a hidden layer of radial units and an output layer of linear units. The hidden layer consists of a set of radial basis functions that act as activation functions whose response varies with the distance between the input and the centre; the distance between two points is given by the difference of their coordinates and by a set of parameters. The RBF is fairly compact, where the linear nature of the radial basis functions reduces computational cost to have a reasonably fast training. The model for the function is a linear combination of a set of weighted basis functions; the prediction

capacity of the network is stored in the weights which can be obtained from a set of training patterns. This process is equivalent to finding a surface in multidimensional space that provides the best fit to the training data, which is then used to interpolate the test data.

### 2.5. Searching of optimum designs

Numerical optimization methods constitute an efficient tool for analyzing the correlations between geometrical parameters and device performance from CFD calculations and for finding their optimum combination. They have been previously applied to optimization problems in areas such as aerodynamic optimization, mechanical and structural design (Vanderplaats 1984). Since micromixing optimization is a non linear problem i.e. a multipeak problem, an exploratory technique has to be used for seeking the global optimum; it evaluates designs throughout the parameter space and only make use of the computation of the objective functions values. In this study, a genetic algorithm has been used due to its capacity to be implemented to solve multi-objective optimization problems. This multi-objective genetic algorithm (MOGA) can converge to a population composed of individuals that belong to the Pareto front of the solutions. To avoid the high number of evaluations of the objective function required to reach an optimum configuration, the actual objective functions are replaced by the approximated functions (response surfaces) built as described in section 2.4.

The Non-dominated Sorting Genetic Algorithm (NSGA-II) (Deb et al 2000) has been applied on the response surfaces with the following parameters values: Population size = 26, Number of generations = 100, Crossover probability = 0.9, Crossover distribution index = 20 and Mutation distribution index = 100. The application pursued the maximization of the Mixing index and the minimization of the Pressure drop.

### 3. Results and analysis

The Mixing index outcomes from CFD at the

outlet section of the mixing channel are shown in figure 3; the results for  $Re = 1$  and  $Re = 10$  keep similar relative values of the Mixing index among the 27 designs and the mixing performance is clearly higher at  $Re = 1$  than at  $Re = 10$ .

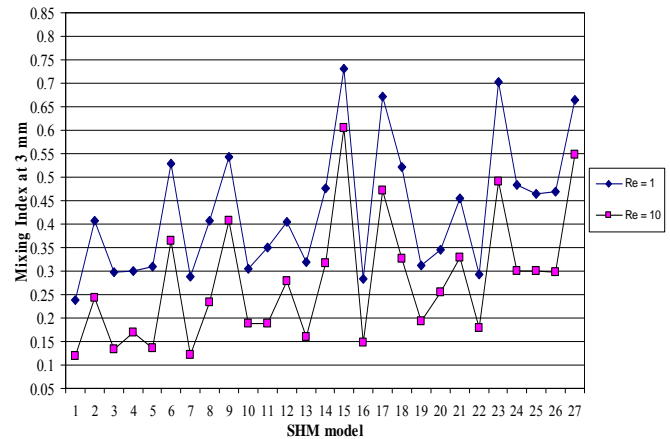


Fig. 3. Mixing index from designs of OA L<sub>27</sub>.

The response surfaces for the performance parameters mixing index and pressure drop are built using the RBF method on the 27 SHM designs of OA L<sub>27</sub>. The values of the design variables (levels in table 1) at these design points and the corresponding objective functions (performance parameters outcomes from CFD solving) are used to train the network. Figure 4 depicts the response surface for mixing index versus two of the design variables.

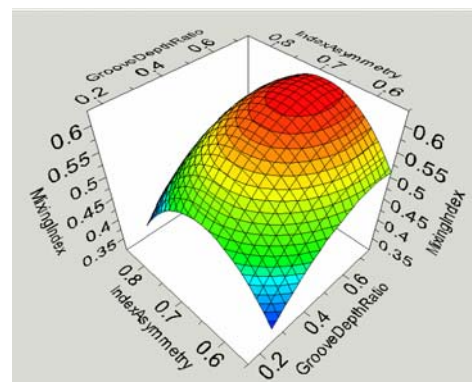


Fig. 4. Response surface generated with RBF.

The results of applying the NSGA-II on the response functions are shown in figures 5a and 5b for  $Re = 1$  and  $Re = 10$  respectively; the

application gives an in-bounded set of optimum designs, i.e. the ranges of the two performance parameters are in the positive zone with coherent values (0 to 1 for Mixing Index and  $>0$  for Pressure drop), for the entire population generated by the genetic algorithm. These results confirm the ranges and levels of the design parameters in table 1 were well selected for the DOE.

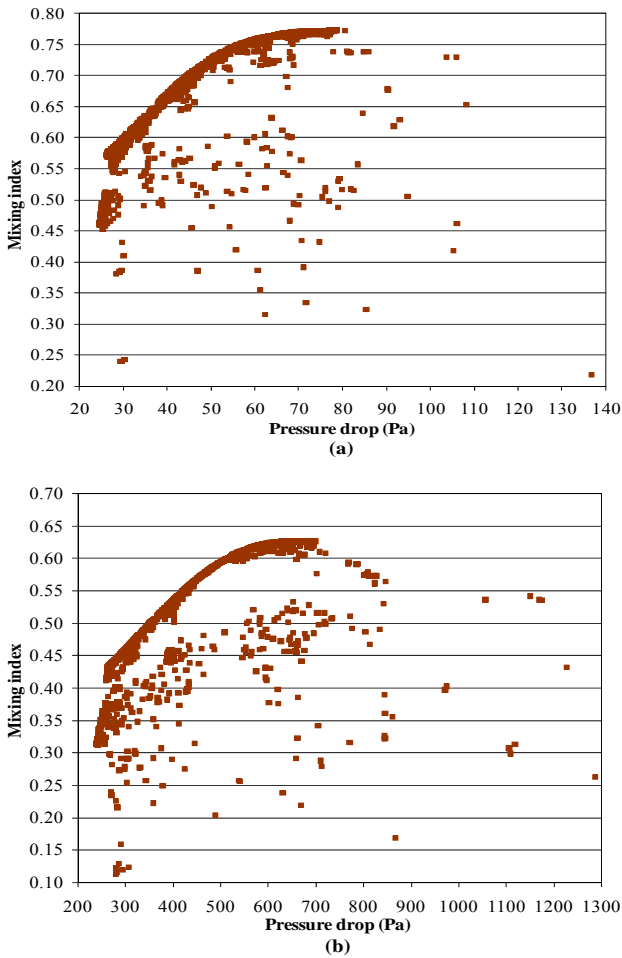


Fig. 5. Results from the application of NSGA-II on RBF approx. functions: (a)  $Re = 1$  (b)  $Re = 10$ .

To validate the numerical optimization, some design points on the Pareto front (Pf) were selected to create the corresponding models for direct numerical solution with CFD at the corresponding Reynolds numbers. In Figure 6, the CFD outcomes are compared to the values predicted by the optimization method. The average differences in percentage between these results is about 3% in mixing index and 1% in pressure drop for  $Re = 1$  and 5% and 1% respectively for  $Re =$

10, which are quite reasonable for the method employed. Figure 6 shows that the optimization technique gives clearly the trend of mixing performance vs. pressure drop in the designs at different  $Re$  numbers; it recreates fairly well the Pareto fronts in figure 5 that correspond to the optimization goal.

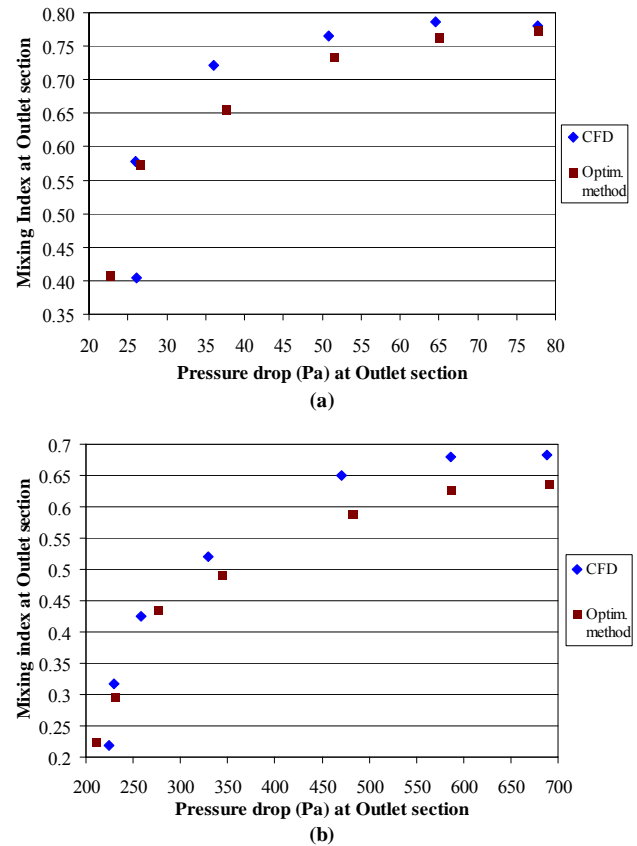


Fig. 6. Mixing Index vs. Pressure drop in selected designs of the Pareto front (a)  $Re = 1$  (b)  $Re = 10$ .

For  $Re = 1$ , the values of the design parameters of six selected optimum designs from the Pareto front are shown in table 3. From these values, one can notice that for most of the selected designs the geometric dimensions that vary significantly are only the height of the channel ( $h$ ) and the depth of the groove ( $d$ ). The aspect ratio of the channel is very influential on the mixing performance but the control of the pressure loss due to the multi-objective optimization do not let it reach the maximum possible value of 3.20 (see table 1). Other design parameters do not change much along the Pf and they tend to the following optimum values:  $d/h = 0.60$ ,  $w_g/D = 0.75$  and  $p = 0.68$ . One can see that very

deep grooves do not necessarily improve mixing and what is important is the ratio  $d/h$  which tends to be constant at 0.60.

**Table 3**  
Design parameters of Pf designs,  $Re = 1$ .

Pf	Params.					
	$W/h$	$d/h$	$w_g/D$	$p$	$Mi$	$\Delta P$ (Pa)
design						
pf1	1.60	0.25	0.75	0.55	0.40	26.09
pf3	1.62	0.60	0.75	0.69	0.58	25.97
pf8	1.91	0.61	0.75	0.67	0.72	36.08
pf13	2.27	0.60	0.75	0.69	0.77	50.86
pf19	2.55	0.60	0.75	0.69	0.79	64.54
pf24	2.73	0.62	0.69	0.68	0.78	77.69

Also, the ratio  $w_g/D$  adopts the highest possible value of 0.75 (see table 1) showing that wide grooves promote higher flow rate inside them which generates the transversal flow that help mixing and also reduce the pressure loss in the system, which is in agreement with the main conclusion of Yang et al (2005); parameter  $p$  tend to be around 0.68 which confirms the finding of Stroock et al (2002) who reported a value of 0.67 makes the transverse flow occupy most of the cross sectional area of the mixing channel.

#### 4. Experimental work

For the optimum designs, experimental tests have been implemented and are in progress to validate the numerical results qualitatively and quantitatively. The SHM models are fabricated by micromachining of polymethylmethacrylate (PMMA) sheets using a CNC router with microtools that can give an accuracy of about 1 micron; two layers (channels and grooves) are formed, aligned and assembled by thermal bonding. The experiments consist on the visualization of streams of colour food dyes for qualitative comparison and streams of de-ionized water used as solvent and aqueous fluorescein solution for quantitative analysis.

Figure 7 shows a combination of simulation concentration contours and experiment images

with red and blue food dyes. The qualitative correspondence between the microscope image and the numerical concentration contours on a plane at half the height of the mixing channel is clear. The upper contours correspond to concentration on a horizontal plane at half the depth of the grooves

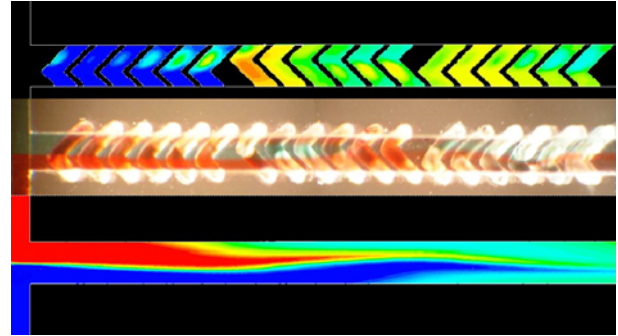


**Fig. 7.** Qualitative comparison between simulation contours and experiment microscope images for the SHM model pf19 (see table 3) at  $Re = 1$ .

The quantitative analysis from experiments with fluorescent dyes is in progress and will be presented in the conference.

#### 4. Conclusions

A numerical design methodology that combines CFD solving with an optimization procedure based on the systematic application of techniques DOE, FA and MOGA was employed to optimize the geometry of the SHM to maximize the mixing performance and minimize the pressure loss in the device. Four design parameters of the SHM were used for a detailed analysis of their effect on the performance of the mixer for which a table of 27 design configurations was created by DOE. The Radial Basis Function (RBF) method was used to create accurate approximated objectives functions (surfaces) that relate the performance parameters to the design parameters. By applying the genetic algorithm NSGA-II on the approximations we could create Pareto front of trade-offs between mixing index and pressure drop. Six and seven different geometries of the micromixer along the Pareto front were selected for Reynolds numbers of 1 and 10 respectively and evaluated with CFD. The resulting

computations confirmed that both the trend and actual values of the mixing index and pressure drop are well predicted by the numerical optimization technique on the response function. Also, experiments are implemented to validate the CFD solutions on the predicted optimum designs.

This optimization approach opens the option to work on the optimization of micromixers for two or more controllable performance parameters that respond to the user requirements. Also the procedure allows the identification of the effect of the geometric features on the performance of the device, that can be used in future designs for specific applications and conditions.

## Acknowledgments

We gratefully acknowledge the Dorothy Hodgkin Postgraduate Award (DHPA) of the Engineering and Physical Sciences Research Council (EPSRC) of United Kingdom and Ebara Research Co. Ltd. of Japan for their financial support.

## References

- Ansari M. A., Kim K. -Y., 2007a. Application of the Radial Basis Neural Network to Optimization of a Micromixer. *Chemical Engineering Technology* 30 (7), 962-966.
- Ansari M. A., Kim K. -Y., 2007b. Shape optimization of a micromixer with staggered herringbone groove. *Chemical Engineering Science* 62, 6687-6695.
- ANSYS Europe Ltd., 2007. CFX 11.0 User Manual.
- Aubin J., Fletcher D. F., Bertrand J., Xuereb C., 2003. Characterization of the mixing quality in micromixers. *Chemical Engineering Technology* 26 (12), 1262-1270.
- Aubin J., Fletcher D. F., Xuereb C., 2005. Design of micromixers using CFD modelling. *Chemical Engineering Science* 60 (8-9), 2503-2516.
- Bonaiuti D., Zangeneh M., 2006. On the coupling of inverse design and optimization techniques for turbomachinery blade design. ASME Paper GT2006-90897. To be published in ASME J. Of Turbomachinery.
- Danckwerts P. V., 1952. The definition and measurement of some characteristics of mixtures. *Appl. Sci. Res. A* 3, 279-296.
- Deb K., Agrawal A., Pratap T, Meyarivan T., 2000. A fast and elitist multi-objective genetic algorithm for multi-objective optimization: NSGA-II. *Proceedings of the Parallel Problem Solving from Nature VI Conference*, pp. 849-858, Paris, France.
- Hassel D. G., Zimmerman W. B., 2006. Investigation of the convective motion through a staggered herringbone micromixer at low Reynolds number flow. *Chem. Eng. Sci.* 61, 2977-2985.
- Hessel V., Lowe H., Schonfeld F., 2005. Micromixers, a review on passive and active mixing principles. *Chem. Eng. Sci.* 60, 2479-2501.
- Kang T. G., Kwon T. H., 2004. Colored particle tracking method for mixing analysis of chaotic micromixers. *Journal of Micromechanics and Microengineering* 14 (7), 891-899.
- Kang T. G., Singh M. K., Kwon T. H., Anderson P. D., 2008. Chaotic mixing using periodic and aperiodic sequences of mixing protocols in a micromixer. *Microfluidics and Nanofluidics* 4 (6), 589-599.
- Kansa E. J., 1999. Motivation for using radial basis function to solve PDE's (unpublished paper), in <http://rbf-pde.uah.edu/kansaweb.html>, accessed on Aug 22<sup>nd</sup>, 2007.
- Li C., Chen T., 2005. Simulation and optimization of chaotic micromixer using lattice Boltzmann method. *Sensors and Actuators B* 106, 871-877.
- Liu Y. Z., Kim B. J., Sung H. J., 2004. Two-fluid mixing in a microchannel. *International Journal of Heat and Fluid Flow* 25, 986-995.
- Lynn N. S., Dandy D. S., 2007. Geometrical optimization of helical flow in grooved micromixers. *Lab on a Chip* 7, 580-587.
- Nguyen N., Wu Z., 2005. Micromixers-a review. *Journal of Micromechanics and Microengineering* 15, R1-R16.
- Ottino J. M., 1989. *The kinematics of mixing: stretching, chaos and transport*. Cambridge University Press. Cambridge.
- Pointwise Inc., 2006. *Gridgen 15.1 User Manual*.
- Singh M. K., Kang T. G., Meijer H. E. H., Anderson P. D., 2008. The mapping method as a toolbox to analyze, design and optimize micromixers. *Microfluidics and Nanofluidics* 5 (3), 313-325.
- Stroock A. D., Dertinger S. K. W., Ajdari A., Mezić I., Stone H. A., Whitesides G. M., 2002. Chaotic mixer for microchannels. *Science* 295, 647-651.
- Stroock A. D., McGraw G. J., 2004. Investigation of the staggered herringbone mixer with a simple analytical model. *Philos. Trans. Royal Soc. London, Ser. A* 362 (1818), 971-986.
- Taguchi G., 1987. *Systems of Experimental Design*, Vols. 1 and 2. New York: Kraus International. NY.
- Vanderplaats G. N., 1984. *Numerical optimization techniques for engineering design: with applications*. McGraw-Hill Book Company, New York.
- Yang J. -T., Huang K. -J., Lin Y. -C., 2005. Geometric effects on fluid mixing in passive grooved micromixers. *Lab on a Chip* 5 (10), 1140-1147.